© 2014. Published by The Company of Biologists Ltd | The Journal of Experimental Biology (2014) 217, 1333-1345 doi:10.1242/jeb.095810

RESEARCH ARTICLE

Role of axial muscles in powering mouth expansion during suction feeding in largemouth bass (*Micropterus salmoides*)

Ariel L. Camp* and Elizabeth L. Brainerd

ABSTRACT

Suction-feeding fishes capture food by fast and forceful expansion of the mouth cavity, and axial muscles probably provide substantial power for this feeding behavior. Dorsal expansion of the mouth cavity can only be powered by the epaxial muscles, but both the sternohyoid, shortening against an immobile pectoral girdle to retract the hyoid, and the hypaxial muscles, shortening to retract both the pectoral girdle and hyoid, could contribute ventral expansion power. To determine whether hypaxial muscles generate power for ventral expansion, and the rostrocaudal extent of axial muscle shortening during suction feeding, we measured skeletal kinematics and muscle shortening in largemouth bass (*Micropterus salmoides*). The three-dimensional motions of the cleithrum and hyoid were measured with X-ray reconstruction of moving morphology (XROMM), and muscle shortening was measured with fluoromicrometry, wherein changes in the distance between radio-opaque intramuscular markers are measured using biplanar X-ray video recording. We found that the hypaxials generated power for ventral suction expansion, shortening (mean of 6.2 mm) to rotate the pectoral girdle caudoventrally (mean of 9.3 deg) and retract the hyoid (mean of 8.5 mm). In contrast, the sternohyoid shortened minimally (mean of 0.48 mm), functioning like a ligament to transmit hypaxial shortening to the hyoid. Hypaxial and epaxial shortening were not confined to the rostral muscle regions, but extended more than halfway down the body during suction expansion. We conclude that hypaxial and epaxial muscles are both crucial for powering mouth expansion in largemouth bass, supporting the integration of axial and cranial musculoskeletal systems for suction feeding.

KEY WORDS: Cleithrum, Hypaxial, Muscle strain, Prey capture, XROMM

INTRODUCTION

Suction feeding in fish requires substantial muscle power to expand the buccal cavity with enough speed to entrain elusive prey, and with enough force to accelerate a bolus of water (e.g. Lauder, 1980; Wainwright and Day, 2007). The cranial muscles may contribute some of this power, but they are probably too small to be the sole source of power (Aerts et al., 1987; Van Wassenbergh et al., 2007a; Carroll and Wainwright, 2009). Instead, the axial body muscles are hypothesized to generate much of the power for suction feeding. The epaxial and hypaxial muscles are large, fast-fibered, capable of high power outputs (Coughlin and Carroll, 2006; Van Wassenbergh et al., 2007b) and attach to elements of the feeding apparatus. Although epaxial muscle power has been demonstrated during suction feeding by measurements of muscle shortening and activity (Carroll and Wainwright, 2006), hypaxial muscle power has only been inferred. There are no direct measurements of hypaxial muscle shortening, so it is unknown whether the hypaxials contribute to suction feeding.

The axial muscles have the potential to power suction feeding because they attach directly to two of the three functional units of expansion (Fig. 1) that drive buccal expansion (Lauder, 1985). The dorsal expansion unit increases the dorsoventral height of the buccal cavity through elevation of the neurocranium relative to the vertebral column (Fig. 1A). Epaxials are the only muscles that span from the vertebral column to the neurocranium (Fig. 2A), and therefore are capable of producing neurocranium elevation. The ventral expansion unit also increases buccal cavity height, through depression and retraction of the lower jaw and hyoid apparatus (Fig. 1B). The hypaxials attach to the pectoral girdle at the cleithrum (Fig. 2C), which is linked to the hyoid apparatus, so these muscles could potentially power ventral expansion (Tchernavin, 1953; Van Wassenbergh et al., 2007a). Cranial muscles, including the sternohyoideus, also have the orientation and attachments necessary to produce ventral expansion (Fig. 2B). The lateral expansion unit increases the mediolateral width of the buccal cavity through abduction of the suspensoria (Fig. 1C). This unit is believed to be powered indirectly by the dorsal and ventral functional units, rather than direct muscle power (Muller, 1989; Aerts, 1991; Van Wassenbergh et al., 2013). Therefore, the muscles powering dorsal and ventral expansion may be the primary sources of power to the lateral unit as well, although this hypothesis remains to be tested. Additionally, a linkage coupling the dorsal and ventral expansion units has been proposed (Muller, 1987), through which the epaxial muscles may contribute power to ventral expansion as well.

The power for suction expansion can only be produced by muscles that actively shorten. Power is the product of force and velocity, so a muscle must generate both force and positive shortening velocity to produce power. Active muscles can produce force without changing length, such as limb muscles supporting the body (Roberts et al., 1997), or produce force while lengthening to absorb energy, as during the landing phase of a jump (Azizi and Abbott, 2013). However, the power required to explosively expand the mouth during suction feeding can only be produced by actively shortening muscles.

Measurements of muscle shortening and activity have demonstrated that epaxial muscles power dorsal expansion (Fig. 2A). The rostral regions of the epaxial muscles are electrically active during suction expansion in many species (reviewed by Lauder, 1985; Westneat, 2005), and in the largemouth bass, *Micropterus salmoides*, they are also shortening and generating power (Carroll and Wainwright, 2006). However, it is unknown how much of the epaxial musculature contributes power for suction expansion. Although activity in the epaxials extends over halfway down the body during feeding (Thys, 1997), muscle shortening has only been measured rostrally.

Department of Ecology and Evolutionary Biology, Brown University, Providence, RI 02912, USA.

*Author for correspondence (ariel_camp@brown.edu)

Received 28 August 2013; Accepted 9 December 2013

The Journal of Experimental Biology (2014) doi:10.1242/jeb.095810

List of abbreviations

ACS	anatomical coordinate system
JCS	joint coordinate system
XROMM	X-ray reconstruction of moving morphology

Unlike dorsal expansion, the ventral expansion unit involves multiple lever systems that transform caudal hyoid motion (retraction) into ventrally directed hyoid depression (e.g. Lauder, 1985; Aerts, 1991). Hyoid retraction is produced when the urohyal translates caudally, causing the more lateral hyoid bars to flare laterally and rotate ventrally (Fig. 1C). Ventral rotation of the hyoid bars produces depression of the hyoid apparatus. These lever systems have been modeled (e.g. Muller, 1989), but there are few direct measurements of hyoid motion because the elements are obscured in standard, visible-light videos.

Two muscles have the orientation and attachments to power ventral expansion through urohyal retraction: the sternohyoid and the hypaxials (Fig. 2B,C). Typically, the sternohyoid muscle is thought to power hyoid retraction (e.g. Lauder and Lanyon, 1980; Carroll and Wainwright, 2006), as this is the only muscle that attaches to the urohyal with an orientation to generate hyoid retraction and is electrically active during suction expansion in many species (reviewed by Westneat, 2005). In largemouth bass, the sternohyoid usually shortened during suction expansion (Carroll, 2004). However, in several catfish species the sternohyoid lengthened during suction expansion (Van Wassenbergh et al., 2007a). Urohyal retraction could also be powered by the hypaxial muscles retracting the cleithrum. Cleithrum retraction may be transmitted to the urohyal through the sternohyoid to produce urohyal retraction (Fig. 2C). Although the cleithrum has been reported to be stable during feeding, implying that the hypaxial muscles are only generating force (e.g. Lauder and Lanyon, 1980), it has been difficult to measure its motion independently from other expansion kinematics. The rostral hypaxials are generally active during suction expansion (e.g. Lauder

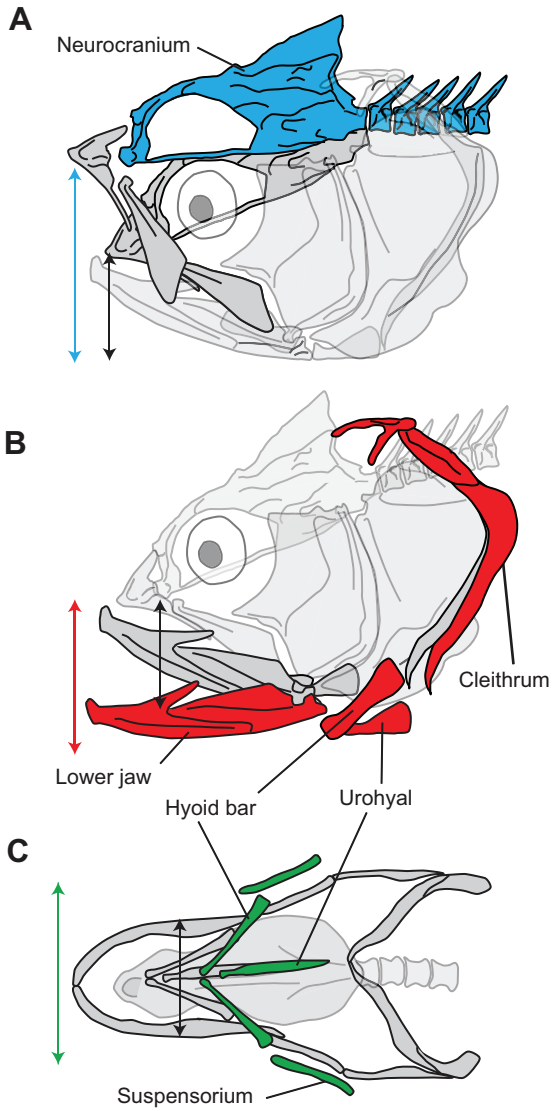

Fig. 1. Bass skeletal components used in feeding. Diagrams of the dorsal (A), ventral (B) and lateral (C) functional units of expansion used during suction feeding. Initial bone positions are shown in gray and expanded positions in color. Black arrows show mouth cavity dimensions at rest, and colored arrows show mouth cavity dimensions (dorsoventral height in A and B and mediolateral width in C) at maximum expansion.

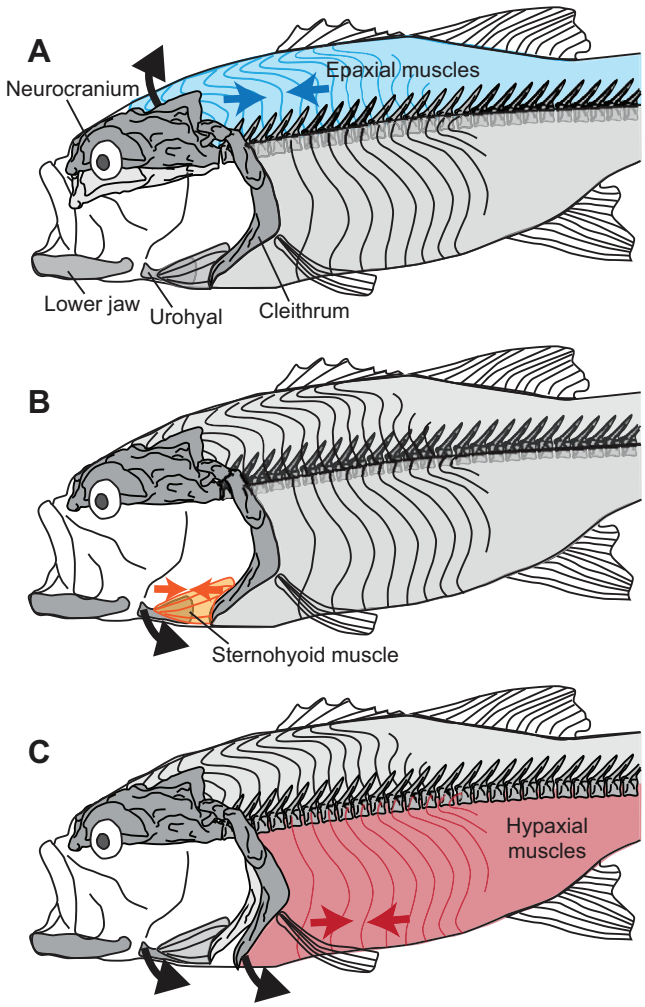

Fig. 2. Hypothesized dorsal and ventral expansion kinematics and the muscles powering them. (A) Dorsal expansion through elevation of the neurocranium and shortening of the epaxial muscles (blue). (B) Ventral expansion through retraction of the urohyal and shortening of the sternohyoid muscle (yellow). (C) Ventral expansion through retraction of the urohyal and cleithrum and shortening of the hypaxial muscles (red). The position of bones at rest is shown in light gray, and position of bones at maximum expansion is shown in dark gray.

and Norton, 1980; Lauder, 1981), but this activity has been hypothesized to anchor the cleithrum, as the hypaxials are presumed not to shorten.

Either the hypaxials or the sternohyoid, or both, can generate power for ventral expansion. If only the sternohyoid muscle contributes power, then the cleithrum should be immobile during suction expansion and the sternohyoid should shorten by the same distance that the urohyal retracts (Fig. 2B). The urohyal and sternohyoid are in line, so the distance that the urohyal is translated caudally should match the distance that the sternohyoid muscle shortens. For sternohyoid shortening to generate translation at its rostral attachment on the urohyal, the muscle's distal attachment site at the cleithrum is expected to be relatively stable. The cleithrum could be anchored by the hypaxials if these muscles are producing force by contracting isometrically.

The hypaxial muscles could power ventral expansion if the cleithrum is rotated caudally and hypaxial shortening and urohyal retraction are equal (Fig. 2C). The hypaxial muscle fibers are in line with the rostrocaudal axis of the urohyal, so urohyal retraction distance should equal the distance the hypaxial muscles shorten, if the hypaxials are generating urohyal retraction. The hypaxial muscles attach directly to the cleithrum, so shortening would rotate the cleithrum caudally (i.e. retract it). Cleithrum retraction would then be transmitted to the urohyal through the sternohyoid muscle, which may be active but undergo little or no shortening (Van Wassenbergh et al., 2007a). Based on musculoskeletal morphology, the hypaxials are the only muscles with the correct attachments and orientation to generate cleithrum retraction. It is conceivable that the sternohyoid could shorten passively (if the cleithrum protracts or if the cleithrum retracts more slowly than the hyoid). However, aside from any hydrodynamic forces generated by incoming water, activity of the hypaxial muscles is the only mechanism for pectoral girdle retraction and hypaxial shortening. Therefore, any hypaxial shortening is presumably active shortening, generating power.

Ventral expansion could also receive power from the epaxial muscles through the hyoid linkage, which couples the dorsal and ventral expansion units. Through this linkage, neurocranium elevation generates elevation of the suspensorium, which in turn causes ventral rotation (i.e. depression) of the hyoid (Muller, 1987; Westneat, 1990). Thus, by powering neurocranium elevation, the epaxial muscles could also generate power for hyoid depression. However, the epaxials cannot power cleithrum retraction: only the hypaxials can produce this motion. If this linkage is the only mechanism of hyoid depression, then the peak magnitudes of both neurocranium elevation and epaxial shortening would be correlated with that of hyoid depression, and the timing of all three events would be synchronous. However, even if peak excursions are not correlated and synchronous, epaxial muscles can still contribute power to ventral expansion during the stage of mouth expansion during which neurocranium elevation and hyoid motion co-occur. Therefore, in addition to the hypaxial and sternohyoid muscles, the epaxials might also contribute power to ventral expansion.

In this study, the role of the epaxial and hypaxial muscles in powering suction expansion was determined during feeding in largemouth bass (*Micropterus salmoides*). Kinematics of the neurocranium, cleithrum and urohyal were measured independently with X-ray reconstruction of moving morphology (XROMM), which combines biplanar X-ray videography with bone models to visualize and measure three-dimensional (3D) skeletal kinematics (Brainerd et al., 2010; Gatesy et al., 2010). Muscle shortening was measured throughout the epaxial and hypaxial muscles and in the sternohyoid muscle with fluoromicrometry, which uses intramuscular radio-opaque markers and X-ray video recording to determine length changes of muscles (e.g. Astley and Roberts, 2012). These kinematic and muscle length data were used to determine: (1) whether the hypaxials and/or the sternohyoid muscle contribute power to ventral expansion; and (2) what is the rostrocaudal extent of muscle shortening in the epaxial and hypaxial muscles during suction expansion.

RESULTS

We were able to measure the magnitudes of dorsal and ventral expansion kinematics independently and combine these with muscle shortening data to determine axial muscle function during suction feeding. To examine the magnitudes of each expansion unit separately (supplementary material Fig. S1), the kinematics of each bone of the dorsal (neurocranium) and ventral (urohyal and cleithrum) expansion units were calculated relative to a body-based reference, the body plane (Figs 3, 4). Anatomical coordinate systems were used to describe the kinematics of each bone as biologically relevant translations and rotations (Brainerd et al., 2010; Dawson et al., 2011; Gidmark et al., 2012), and the motion of each bone

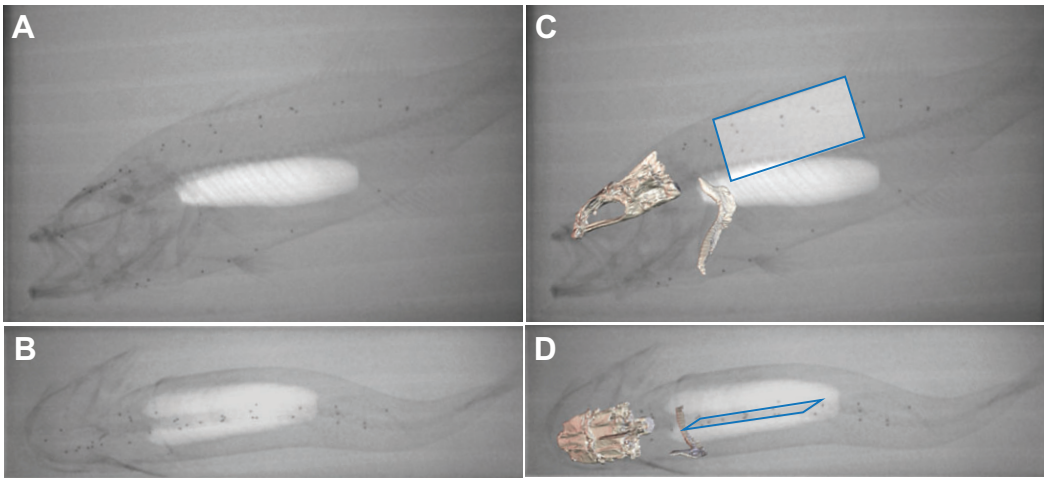

Fig. 3. X-ray video frames of suction feeding. Lateral-view (A,C) and ventral-view (B,D) X-ray video frames from a representative strike at peak cleithrum retraction. In C and D, animated bone models and the body plane model (blue outline) have been superimposed on the X-ray frames using X-ray reconstruction of moving morphology (XROMM).

The Journal of Experimental Biology (2014) doi:10.1242/jeb.095810

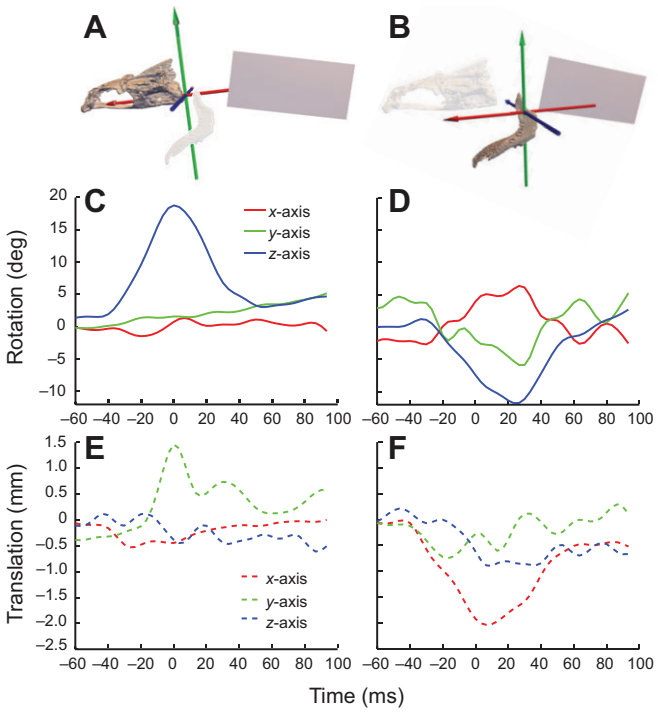

Fig. 4. Skeletal kinematics during feeding. Joint coordinate systems (JCSs) and sample six-degree-of-freedom kinematics of the neurocranium (A,C,E) and cleithrum (B,D,F). Rotations (C,D) and translations (E,F) are shown for each bone. Axes follow right-hand rule, so for the neurocranium positive *z*-axis rotation corresponds to elevation, and for the cleithrum negative *z*-axis rotation corresponds to cleithrum retraction. All kinematics for each bone were calculated relative to the body plane, and zero rotation and translation corresponds to the position of the bone prior to the onset of the strike. The colors of the JCS axes in A,B are the same as those used in the graphs in C–F: *x*-axis, red; *y*-axis, green; and *z*-axis, blue. Time is relative to the time of peak neurocranium elevation.

relative to the body plane was described with a joint coordinate system (see Materials and methods section). General patterns were consistent, but there was substantial variation in the magnitude of shortening and kinematic variables both within and among individuals, although only for a few variables was the effect of individual significant. Therefore, pooled means are reported in the text, except where noted, but Tables 1 and 2 show both individual and pooled means.

Suction feeding behavior

Suction feeding strikes in all fish often included substantial lateral motion of the head and body (Fig. 3B,D; also see supplementary material Movie 1). Lateral expansion of the mouth cavity could clearly be seen, but was not the focus of this study. The fish used a beat of the caudal fin to accelerate towards the prey, and then abducted the pectoral fins and oriented the head towards the prey just before the onset of mouth opening. Often this orientation resulted in the head being laterally rotated to one side, relative to the body plane, so that the fish had a C- or S-shaped posture during suction expansion (see supplementary material Movie 1).

Skeletal kinematics from XROMM

During suction expansion the cleithrum was retracted, rotating caudoventrally (about a mediolateral axis) relative to the body plane. Cleithrum rotation was captured in our joint coordinate system primarily as negative *z*-axis rotation (Fig. 4B,D). As with all kinematic variables, *z*-axis rotation magnitude was calculated relative to the *z*-axis rotation prior to the onset of the strike. Peak *z*-axis rotation averaged −9.3 deg (Table 1), and occurred after maximum neurocranium elevation (Fig. 5A–C), although the timing varied significantly among individuals (ANOVA, $F_{2,27}$=3.6, P=0.04). Peak *z*-axis rotation occurred 14±3.0, 23±1.7 and 20.3±2.4 ms after peak neurocranium elevation in Bass01, Bass02 and Bass03, respectively (means ± s.e.m.; N=10 strikes per individual).

There was some negative *y*-axis (i.e. lateral) rotation of the cleithrum in all fish (Fig. 5A–C), with a mean peak magnitude of −8.7 deg (Table 1). The *y*-axis rotation usually reached its peak after *z*-axis rotation, but the timing varied substantially with significant differences among individuals (ANOVA, $F_{2,27}$=4.9, P=0.019). Peak *y*-axis rotation occurred 88±33.7, −3±7.4 and 12±16.3 ms after peak cleithrum retraction in Bass01, Bass02 and Bass03, respectively (means ± s.e.m.; N=10 strikes per individual). Cleithrum translations were small (Table 1), but included a negative *x*-axis (i.e. caudal) translation, with a mean peak magnitude of −1.8 mm (Fig. 5D–F).

As expected, the neurocranium was elevated during suction expansion, rotating caudodorsally (about a mediolateral axis), relative to the body plane. Neurocranium elevation was described primarily as positive *z*-axis rotation in our joint coordinate system

Table 1. Mean peak magnitudes of skeletal kinematics for each individual and for pooled data from all individuals

		Bass01	Bass02	Bass03	Pooled
Bone		Mean peak ± s.e.m.	Mean peak ± s.e.m.	Mean peak ± s.e.m.	Mean peak ± s.e.m.
Cleithrum	*x*-translation (mm)	−1.58±0.5	−1.53±0.3	−2.32±0.7	−1.81±0.3
	y-translation (mm)	−0.59±0.14	−0.67±0.2	−0.47±0.2	−0.58±0.1
	z-translation (mm)	1.88±0.3	0.82±0.3	1.20±0.5	1.30±0.2
	x-rotation (deg)	8.52±1.9	4.29±0.7	2.85±0.7	5.22±0.8
	y-rotation (deg)	−9.74±1.7	−6.79±1.4	−9.67±1.5	−8.73±0.9
	z-rotation (deg)	−7.19±1.2	−10.07±1.7	−10.62±1.2	−9.29±0.8
Neurocranium	*x*-translation (mm)	−0.31±0.1	−0.74±0.1	−0.62±0.2	−0.56±0.1
	y-translation (mm)	1.56±0.2	2.72±0.3	3.30±0.4	2.53±0.2
	z-translation (mm)	1.98±0.43	1.23±0.40	2.25±0.94	1.82±0.4
	x-rotation (deg)	1.85±0.4	1.89±0.37	3.25±0.8	2.33±0.3
	y-rotation (deg)	7.33±1.8	4.71±1.3	3.21±1.0	5.09±0.9
	z-rotation (deg)	12.12±1.28	16.50±1.0	19.25±0.95	15.96±0.8
Urohyal	*x*-translation (mm)	−7.33±0.70	−8.90±1.6	−9.20±1.4	−8.48±0.7
	y-translation (mm)	−7.54±0.3	−8.98±1.0	−10.49±1.0	−9.00±0.5
	z-translation (mm)	−4.16±1.3	−3.77±0.8	−4.05±0.9	−3.99±0.6

N=10 strikes per variable for each individual; N=30 strikes per variable for pooled data.

The Journal of Experimental Biology (2014) doi:10.1242/jeb.095810

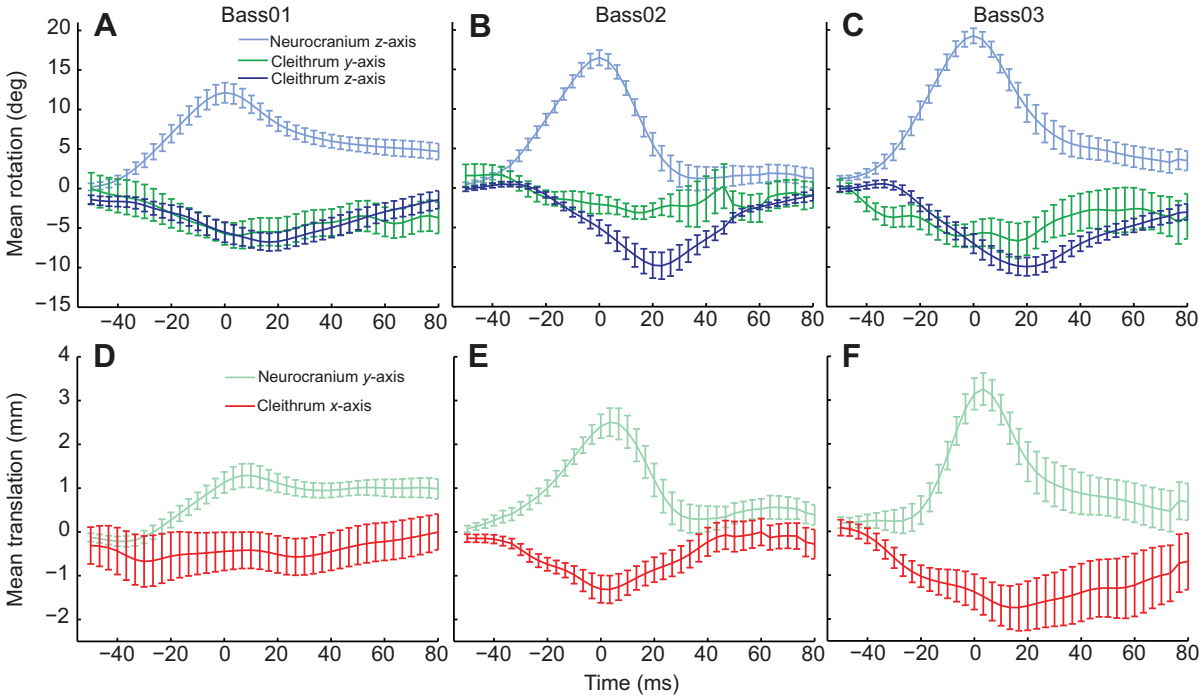

Fig. 5. Skeletal rotations and translations. Mean (±s.e.m.) of selected rotations (A–C) and translations (D–F) of the neurocranium and cleithrum for each individual. For all kinematic variables, time is relative to peak neurocranium elevation. For each individual, all strikes were aligned at time=0 and the mean rotation and translation value calculated at each time step. *N*=10 strikes per individual for most time points. Because not all strikes were recorded for the full length of time (60 ms before peak neurocranium elevation to 80 ms after), some of the first and last mean values in the time sequence were calculated from eight or nine strikes.

(Fig. 4A,C). Peak *z*-axis rotation averaged 16 deg, significantly greater than that of the cleithrum (ANOVA, $F_{2,27}$=624.8, P<0.0001; *t*-test, P<0.0001; Fig. 5A–C). In contrast, *y*- and *x*-axis rotations of the neurocranium were small with mean peaks of 5.1 deg and 2.3 deg, respectively (Table 1). Translations of the neurocranium were small (Table 1), although there was a consistent positive *y*-axis (i.e. dorsal) translation with a mean peak of 2.5 mm (Fig. 5D–F).

The urohyal marker moved both caudally and ventrally during suction expansion, relative to the body plane (Fig. 6). This motion was captured by our anatomical axis as negative *x*-axis (i.e. caudal) and negative *y*-axis (i.e. ventral) translations, with mean peak values of −8.5±0.7 and −9.0±0.7 mm (means ± s.e.m.; N=30 strikes), respectively. The peak magnitudes of urohyal retraction and depression were each significantly and linearly correlated with the peak magnitude of cleithrum retraction (Pearson's correlations, r=0.87, P<0.01 and r=0.85, P<0.01 for urohyal depression and retraction, respectively) across N=30 strikes from all individuals. The *z*-axis (i.e. mediolateral) translations of the urohyal were small (Table 1). Peak urohyal *x*- and *y*-axis translations occurred at −1.7±1.0 and 2.0±2 ms, respectively, relative to peak cleithrum retraction (Fig. 7). These values did not differ significantly from each other (ANOVA, $F_{1,27}$=2.52, P=0.12) or from zero (single-sample *t*-test, t=0.15, P=0.88).

Fluoromicrometry: whole-muscle strain

We used fluoromicrometry to measure shortening across the hypaxials – from the cleithrum to the caudal edge of the anal fin – and found that these muscles shortened substantially during suction feeding. In the strike shown in Fig. 8, the hypaxials shorten to about 0.88 of their normalized length, representing a 12% strain. These

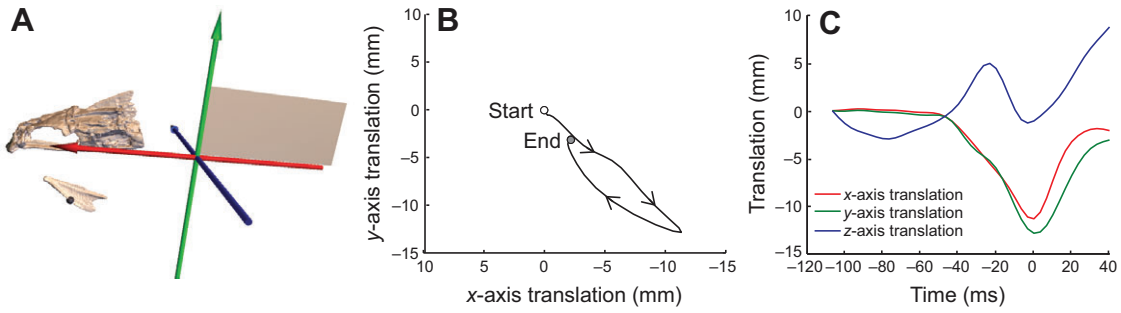

Fig. 6. Anatomical coordinate system (ACS) and sample kinematics of the urohyal. Translations of the urohyal marker were calculated relative to the body plane using the ACS (A), with *x*-axis in red, *y*-axis in green, and *z*-axis in blue. (B) Urohyal motion is shown as *x*- and *y*-axis translations, with the initial position (white circle) and final position (gray circle) indicated and the direction of movement shown with arrows. Zero rotation and translation corresponds to the position of the bone prior to the onset of the strike. (C) The same urohyal motion as in B is also shown as translations over time (with time zero at peak cleithrum retraction). Colors correspond to the axes in A.

The Journal of Experimental Biology (2014) doi:10.1242/jeb.095810

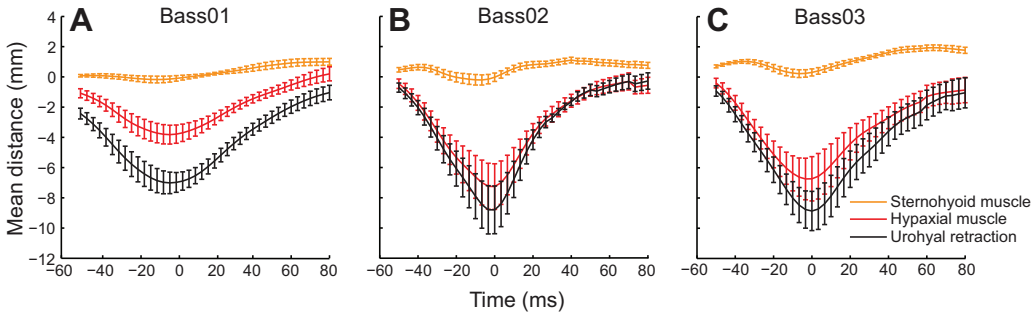

Fig. 7. Mean (±s.e.m.) hypaxial (red) and sternohyoid (yellow) muscle shortening distance and mean urohyal retraction (black). (A–C) For each individual shortening distance was calculated as the change in length relative to the length of the muscle prior to the onset of the strike, with negative distance values corresponding to muscle shortening. Urohyal retraction was measured as negative *x*-axis translation of the urohyal marker, relative to the body plane. Time is relative to peak cleithrum retraction. For each individual, all strikes were aligned at time=0 and the mean translation and shortening values calculated at each time step. *N*=10 strikes per individual for most time points. Because not all strikes were recorded for the full length of time (60 ms before peak cleithrum retraction to 80 ms after), some of the first and last mean values in the time sequence were calculated from eight or nine strikes.

muscles consistently underwent positive strain (i.e. shortening) relative to their length prior to the onset of each strike. The hypaxials had the greatest maximum strain [ANOVA, $F_{2,27}$=32.8, P<0.0001; Tukey's honest significant difference (HSD) P<0.001] and shortening (ANOVA, $F_{2,27}$=41.5, P<0.0001; Tukey's HSD P<0.01) magnitudes of the three muscles (Fig. 9) with mean maximum strain of 7.7±0.9% and shortening distance of 6.2±0.8 mm (means ± s.e.m.; N=30 strikes). Relative to the time of peak neurocranium elevation, the time of maximum hypaxial strain was significantly different from zero (single-sample t-tests, t=12.5, P<0.0001), occurring an average of 16.6±2 ms after peak neurocranium elevation. However, relative to the time of peak cleithrum retraction, the time of maximum hypaxial strain was −2.5±1.4 ms, which was not significantly different from zero (single-sample t-test, t=−1.8, P=0.08).

Hypaxial muscle shortening distance generally matched urohyal retraction (*x*-axis translation), whereas the sternohyoid muscle shortened by a much smaller distance (Fig. 7). Maximum hypaxial shortening magnitude was significantly different from the magnitude of maximum urohyal *x*-axis translation (paired t-test, t-ratio=−7.24, P<0.001). However, the mean difference between hypaxial shortening and urohyal translation was relatively small: 3.3±0.3 mm for Bass01, 1.5±0.5 mm for Bass02 and 2.0±0.7 mm for Bass03 (means ± s.e.m., N=10 strikes each). Peak sternohyoid shortening distance was also significantly less than peak urohyal retraction (paired t-test, t-ratio=−7.24, P<0.0001), and the mean difference was 7.2 mm across all three individuals. Maximum hypaxial shortening magnitude was significantly and linearly correlated with both urohyal peak retraction (Pearson correlation, r=0.92, P<0.01) and peak depression (Pearson correlation, r=0.84, P<0.01) magnitudes across N=30 strikes from all individuals.

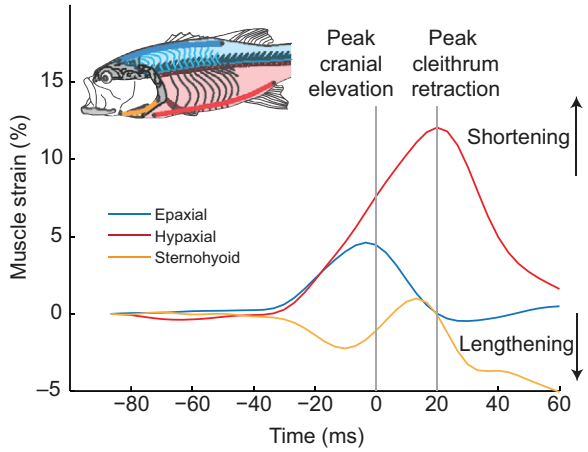

Fig. 8. Sample whole-muscle strains for the epaxial (blue), hypaxial (red) and sternohyoid (yellow) muscles during one strike. Muscle strain was calculated relative to the muscle length measured prior to the onset of the strike, with positive strain values indicating muscle shortening. Time is relative to peak neurocranium elevation, and both the time of peak neurocranium elevation and the time of peak cleithrum retraction are indicated by the gray lines.

The sternohyoid muscle usually shortened during suction expansion, but with low strain magnitudes and variable timing. Sternohyoid length was measured as the distance between markers in the urohyal and cleithrum, because these bones are the rostral and caudal attachments (respectively) of this muscle. In many strikes, the sternohyoid muscle lengthened prior to shortening (Fig. 8) and in some strikes the muscle exclusively lengthened. On average, the sternohyoid did shorten in all individuals (Table 2, Fig. 9), but the magnitude was statistically significantly lower than that of the hypaxial and epaxial muscles, both in maximum strain (ANOVA, $F_{2,27}$=32.8, P<0.0001) and absolute shortening distance (ANOVA, $F_{2,27}$=41.5, P<0.0001). Mean maximum sternohyoid strain was 1.3±0.3% and mean maximum shortening distance was 0.48±0.1 mm. The time of maximum sternohyoid shortening was highly variable, with a mean time of 55.4±12.7 ms (means ± s.e.m.; N=30 strikes) prior to peak cleithrum retraction.

Epaxial muscle length was measured from the neurocranium to the caudal edge of the first dorsal fin using fluoromicrometry. This muscle was found to shorten concurrently with neurocranium elevation (Fig. 8), but with strain magnitudes significantly lower than those of the hypaxials (ANOVA, $F_{2,27}$=32.8, P<0.0001; Tukey's HSD, P=0.0007). Peak epaxial shortening did vary significantly among individuals (ANOVA, $F_{2,27}$=18.98, P<0.0001), with mean maximum shortening distances of 2.5±0.3, 4.0±0.3 and 5.2±0.3 mm for Bass01, Bass02 and Bass03, respectively (means ± s.e.m.; N=10 strikes per individual; Fig. 9). Relative to the time of peak neurocranium elevation, maximum epaxial shortening occurred at −0.44±0.4 ms, which did not differ significantly from zero (single-sample t-test, t=−1.0, P=0.326).

Fluoromicrometry: regional muscle strain

Regional strain measurements revealed a generally consistent pattern of rostrocaudal variation in strain magnitude for each axial muscle. Hypaxial muscles were measured across five regions and

The Journal of Experimental Biology (2014) doi:10.1242/jeb.095810

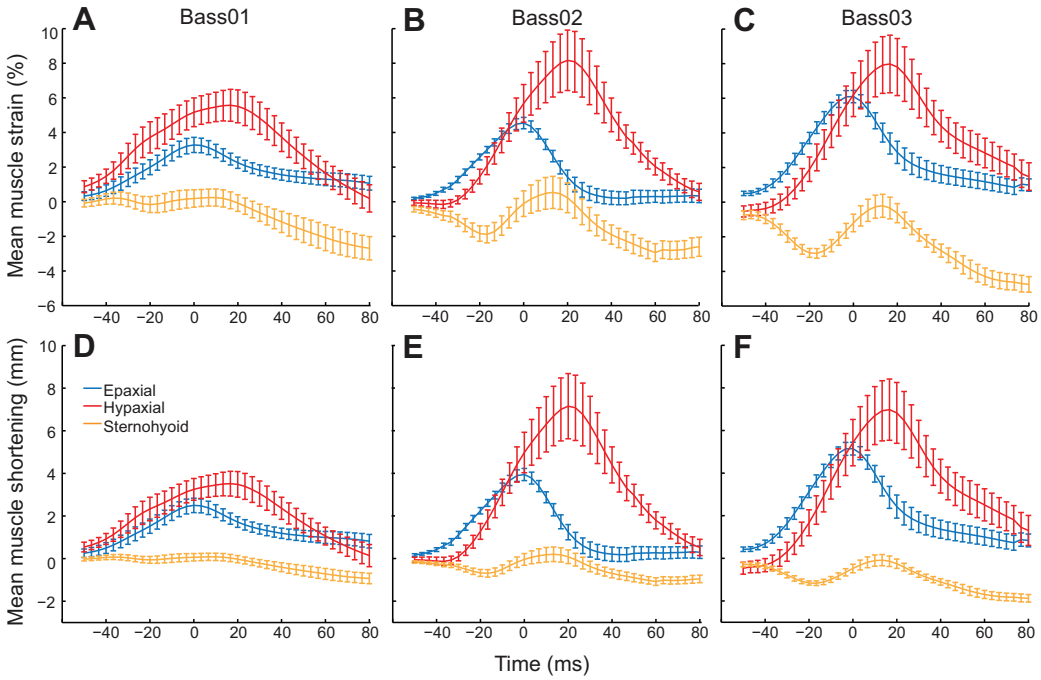

Fig. 9. Mean (±s.e.m.) strain and shortening of the epaxial (blue), hypaxial (red) and sternohyoid (yellow) muscles. (A–F) For each individual both strain (A–C) and shortening (D–F) distance were measured relative to the muscle length prior to the onset of the strike, with positive strain and shortening values corresponding to muscle shortening. Time is relative to peak neurocranium elevation. For each individual, all strikes were aligned at time=0 and the mean strain and shortening value calculated at each time step. *N*=10 strikes per individual for most time points. Because not all strikes were recorded for the full length of time (60 ms before maximum neurocranium elevation to 80 ms after), some of the first and last mean values in the time sequence were calculated from eight or nine strikes.

shortened throughout the four precaudal regions, from the cleithrum to the rostral edge of the anal fin (Fig. 10B). The magnitude of strain in each region varied between individuals at a marginally significant level (ANOVA, $F_{2,17}$=2.99, *t*-tests P=0.05), but all three fish showed a similar pattern of regional strain. Strain magnitudes within the hypaxials varied rostrocaudally (ANOVAs, $F_{4,9}$=18.8, 10.0 and 11.2 for Bass01, Bass02 and Bass03, respectively; P<0.001 for all), with the rostral two to three regions having significantly greater strain than the caudal 1 to 2 regions (Tukey's HSD, P<0.001).

The epaxials were measured across eight regions, and also shortened throughout nearly all of the precaudal regions, from about the craniovertebral joint to the rostral edge of the second dorsal fin (Fig. 10A). Strain magnitudes differed significantly between individuals (ANOVA, $F_{2,23}$=20.36, P=0.0001) and regions (ANOVA, $F_{6,23}$=129.14, P<0.0001). For Bass01 and Bass02, the largest strains were located in the rostralmost region and midbody (fourth most rostral) regions. In Bass03, the strains in the midbody (third and fourth most rostral) regions were significantly greater than those in the rostral or caudal regions (Tukey's HSDs, P<0.0001). Interestingly, both Bass02 and Bass03 had bilateral lengthening (i.e. negative strain) in the caudalmost epaxial regions (Fig. 10A).

DISCUSSION

Our kinematic and muscle shortening data demonstrate that the hypaxial muscles generate power for hyoid depression – and therefore ventral expansion – in largemouth bass. The hypaxial and sternohyoid muscles have each been hypothesized to power ventral expansion (Carroll, 2004; Van Wassenbergh et al., 2007b). However, these competing hypotheses have never been tested in a single species because of the difficulty of measuring muscle shortening and ventral expansion kinematics. We used fluoromicrometry and XROMM to measure shortening in the hypaxial and sternohyoid muscles, as well as the kinematics of the cleithrum and urohyal. The resulting hyoid retraction and hypaxial shortening data demonstrate that the hypaxials, but not the sternohyoid, contributed power to ventral expansion in our largemouth bass.

Hypaxial power for ventral expansion

Our conclusion of hypaxial power generation in largemouth bass is based on the congruence between our urohyal translation and hypaxial muscle shortening distances. If the hypaxials actively shorten to power hyoid retraction, then the distance of hypaxial shortening should match the distance of urohyal retraction. Retraction of this median hyoid element generates hyoid depression through a linkage with the hyoid bars (Aerts, 1991), and we measured its caudal (retraction) and ventral (depression) translation, relative to the body plane (Fig. 6). Maximum urohyal retraction and maximum hypaxial shortening matched in timing (Fig. 7) and were similar in magnitude (mean of 8.5 mm and 6.2 mm, respectively, across individuals). Although peak hypaxial shortening distance was slightly less than urohyal retraction, the difference was relatively small (Fig. 7). These results are consistent with hypaxial muscles

Table 2. Mean maximum muscle shortening and strain magnitudes for each individual and for pooled data from all individuals

		Bass01	Bass02	Bass03	Pooled
Muscle		Mean peak ± s.e.m.	Mean peak ± s.e.m.	Mean peak ± s.e.m.	Mean peak ± s.e.m.
Hypaxials	Strain (%)	6.42±1.0	8.41±1.7	8.29±1.8	7.71±0.9
	Shortening (mm)	4.04±0.6	7.36±1.5	7.25±1.5	6.22±0.9
Sternohyoid	Strain (%)	1.46±0.5	1.54±0.7	0.88±0.4	1.29±0.3
	Shortening (mm)	0.51±0.2	0.57±0.3	0.35±0.1	0.48±0.1
Epaxials	Strain (%)	3.30±0.4	4.57±0.3	6.14±0.35	4.67±0.3
	Shortening (mm)	2.51±0.34	3.97±0.28	5.19±0.30	3.89±0.2

N=10 strikes per variable for each individual; *N*=30 strikes per variable for pooled data.

The Journal of Experimental Biology (2014) doi:10.1242/jeb.095810

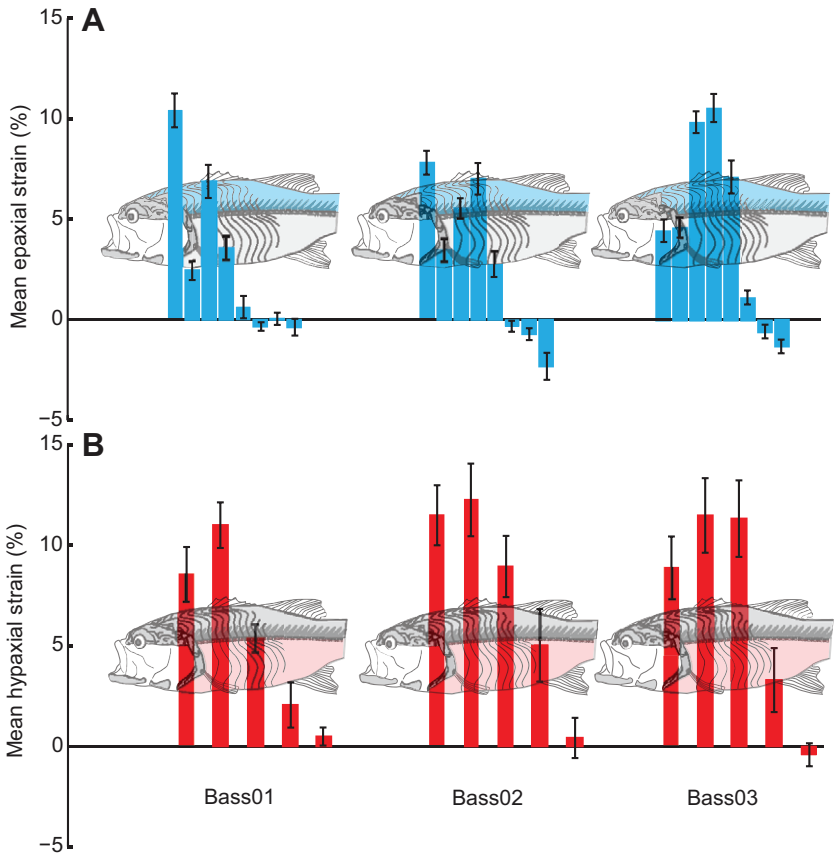

Fig. 10. Mean (±s.e.m.) percentage strain. Strain was measured at time zero in epaxial (A) and hypaxial (B) regions for each individual (*N*=10 strikes). Each bar represents a region of the musculature, the approximate anatomical position of which is indicated by the fish diagrams. Mean epaxial strain for each region is based on the mean of left- and right-side muscle strains at each region. For epaxial regions, time zero is at peak neurocranium elevation, and for hypaxial regions time zero is at peak cleithrum retraction.

actively shortening to produce cleithrum retraction, which is then transmitted to the urohyal through the sternohyoideus to generate hyoid retraction and depression.

We found that the sternohyoid muscle did not generate substantial power for hyoid retraction in our largemouth bass, but instead transmitted hypaxial power to the urohyal. The sternohyoid muscle is active during suction expansion in many species, including largemouth bass (Carroll, 2004), leading to the hypothesis that it actively shortens against a stable cleithrum to power hyoid retraction. However, we measured a mean urohyal retraction of 8.5 mm, whereas the sternohyoid muscle only shortened by a mean of 0.48 mm. This limited shortening suggests a ligament-like function of the sternohyoid in largemouth bass, as has been proposed for the sternohyoid of clariid catfishes (Van Wassenbergh et al., 2007b). Because muscle force production is proportional to muscle cross-sectional area, the sternohyoid muscle in largemouth bass may be too small to generate enough force to shorten against the hypaxial muscles, and therefore cannot contribute power to suction expansion. Our data suggest that the sternohyoid muscle is under tension from cleithrum retraction while it is active, preventing the muscle from shortening and possibly causing intramuscular strain heterogeneity. Strain heterogeneity could explain the discrepancy between the whole-muscle strains measured here (mean of 1.3%) and the intramuscular strains measured previously (mean of 11%) in largemouth bass (Carroll, 2004). However, even an 11% strain throughout the whole sternohyoid would only produce about 4 mm of shortening, which would still not produce the observed urohyal retraction.

Although hypaxial shortening is sufficient to generate the observed hyoid retraction and depression, epaxial muscle power may also contribute to ventral expansion through the hyoid linkage. The epaxial muscles cannot be the sole source of ventral expansion power, as there was a nearly 20 ms offset between peak neurocranium elevation and peak urohyal retraction (Fig. 8). However, epaxial muscle power may contribute to hyoid motion during the first half of ventral expansion, when the neurocranium is elevating (Fig. 5A–C) and the epaxials are shortening (Fig. 9A–C). Even though the XROMM data allow us to measure the kinematics of dorsal and ventral expansion separately (supplementary material Fig. S1), we cannot separate the contributions of epaxial and hypaxial muscles to powering ventral expansion. Therefore, in addition to the hypaxials, the epaxials may also be generating power for ventral expansion.

Cleithrum kinematics

Hypaxial muscle activity has been observed during suction feeding in many species (e.g. Lauder and Norton, 1980; Lauder, 1981), but it was proposed that these muscles act to stabilize the cleithrum rather than to retract it (Lauder, 1982). Until now it was difficult to test this hypothesis because cleithrum kinematics must be measured relative to a reference frame that moves with the fish, but is not involved in suction expansion. In this study, we directly measured cleithrum retraction during suction expansion using our XROMM animations. Previous high-speed video studies have used the neurocranium as a reference, but the resulting measurement will include both neurocranium and cleithrum motion. Instead, we created a body plane fitted to six mid-sagittal epaxial markers (Fig. 3C,D) that moves with the same orientation and translation as the fish, but is largely independent of suction expansion kinematics, and so provides a fish-based reference. We measured cleithrum motion relative to the body plane using a joint coordinate system (Fig. 4B), which allowed us to capture only motion of the cleithrum and to measure retraction independently from other motions of this bone.

The Journal of Experimental Biology (2014) doi:10.1242/jeb.095810

We found that the cleithrum primarily moves caudoventrally during suction expansion, powered by hypaxial muscle shortening. The cleithrum was retracted (i.e. *z*-axis rotation relative to the body plane) by a mean of 9.3 deg across all three bass. The hypaxials are the only muscles with the appropriate orientation and attachments to produce this retraction, and the timing of peak cleithrum retraction and peak hypaxial shortening were nearly coincident (Fig. 8). The cleithrum also rotated about its long axis (i.e. *y*-axis rotation), suggesting that it rotates medially as it is retracted (Fig. 5). These rotations presumably result from motion about the joints of the pectoral girdle, whose functions are largely unknown (but see Gosline, 1977). Although this was not the focus of our study, for one individual we confirmed that there was motion at least at the cleithrum–supracleithrum joint during cleithrum retraction.

This study demonstrates cleithrum retraction in largemouth bass, and pectoral girdle motion during suction expansion may also occur in other species. Cleithrum motion was observed during suction feeding in three species of clariid catfishes: *Clarias gariepinus*, *Gymnallabes typus* and *Channallabes apus* (Van Wassenbergh et al., 2007b). Because of this, hypaxial shortening in these species has been hypothesized (Van Wassenbergh et al., 2005), but not measured. Cleithrum retractions of 4–9 deg have been measured during prey processing in several salmonids and osteoglossomorphs (Sanford, 2001; Konow and Sanford, 2008). The magnitudes of these cleithrum motions may not be directly comparable with those reported here, as previous studies used planar video and measured cleithrum rotation relative to the neurocranium. More measurements of pectoral girdle kinematics, made relative to a body reference, are needed to determine whether cleithrum retraction is widespread in suction feeding fishes.

Epaxial power for dorsal expansion

Our data join previous studies in demonstrating that epaxial muscles are elevating the neurocranium, and therefore powering dorsal expansion in largemouth bass. We found that maximum epaxial shortening (mean of 3.9 mm) was concomitant with maximum neurocranium elevation (Fig. 9). The magnitude of neurocranium elevation measured here is similar to that found in previous studies of this species (Svanbäck et al., 2002), although our muscle strains are less than those reported by Carroll and Wainwright (mean of 4.7% versus 9%, respectively) (Carroll and Wainwright, 2006). However, previous measurements were made over a relatively small (8–12 mm) region of rostral epaxial muscles, whereas our measurements spanned over half the length of the epaxials. Additionally, we found that regional strains often exceeded those of the whole muscle. Overall, both our skeletal kinematics and muscle shortening data are consistent with epaxial muscles powering neurocranium elevation.

The small epaxial strain magnitudes, relative to those of the hypaxial muscles, may reflect the different skeletal levers on which each muscle acts. Neurocranium elevation is often modeled as a lever system (e.g. Carroll et al., 2004) with the fulcrum just caudal to the craniovertebral joint, the rostrocaudal length of the neurocranium as the out-lever, and the dorsoventral height from the craniovertebral joint to the attachment point of epaxial muscles to the neurocranium as the in-lever. The long out-lever length allows relatively small epaxial strains to produce substantial neurocranium elevation. In contrast, the hypaxial muscles attach along the length of the cleithrum and hypaxial shortening directly produces cleithrum retraction. Because there is no lever system to amplify displacement, hypaxial shortening magnitudes need to be greater than those of the epaxial muscles to produce a similar amount of motion.

Rostrocaudal extent of axial muscle shortening

Not only are the epaxial and hypaxial muscles powering dorsal and ventral expansion in largemouth bass, but we also found that power production in these muscles extends far beyond the rostral regions. Previous studies only considered the rostralmost regions of the epaxials to contribute suction expansion power. However, muscle shortening had not been measured in the more caudal regions of the epaxials, or in any region of the hypaxials. Using fluoromicrometry, we measured epaxial and hypaxial muscle shortening throughout almost the entire precaudal region, from the craniovertebral joint and cleithrum to the second dorsal fin and the anal fin (Fig. 10). Epaxial muscle activity does indeed extend this far during suction feeding in largemouth bass (Thys, 1997), and we presume that hypaxial shortening is also active, although muscle activity measurements are needed. Additionally, we cannot deduce either the timing or magnitude of muscle force production from our data. The magnitude of power cannot be calculated without measurements of muscle force, so we can conclude that the axial muscles do generate power during suction feeding, but cannot determine the magnitude of that power. However, muscle power production is generally proportional to muscle mass, so these large axial muscles have the potential to contribute substantial power.

The delay of hypaxial shortening relative to epaxial shortening (see Results) reflects the offset in timing between dorsal and ventral expansion kinematics. Hypaxial shortening occurs over the same duration as urohyal depression and retraction (Fig. 7), and reaches a peak concomitantly with cleithrum retraction (Fig. 8). However, these ventral expansion kinematics occur after neurocranium elevation, so the hypaxials continue to shorten after the epaxials have begun re-lengthening. This timing offset is part of the anterior-to-posterior wave of expansion typical of suction-feeding fishes (e.g. Bishop et al., 2008).

The axial muscles are crucial for suction expansion in largemouth bass, but we need a better understanding of how these muscles produce and transmit expansion power. In this study, we measured muscle length at intervals along the epaxials and hypaxials (Fig. 10), treating them each as a single, homogenous muscle. However, these segmented muscles are made up of myomeres, each with multiple regions of distinctly oriented muscle fibers (Gemballa and Vogel, 2002) and activity patterns that can vary within and between myomeres (Jayne and Lauder, 1995; Thys, 1997). This complexity might be reflected in the heterogeneity of strain magnitude that we observed across the hypaxial and epaxial muscles. In the hypaxials, the greatest strains were concentrated rostrally, whereas in the epaxials the region of greatest strain varied depending on the individual (Fig. 10). This study emphasizes the importance of these muscles during feeding behaviors, as well as our need to better understand how they generate and transmit power.

Although our results demonstrate that axial muscles power dorsal and ventral expansion in largemouth bass, other species may employ different combinations of skeletal kinematics and muscle power to achieve suction expansion. The diversity of feeding apparatus morphology in ray-finned fishes (e.g. Westneat, 2005) may lead to differences in which muscles power ventral expansion, and in the relative importance of each expansion unit. For example, the sternohyoid muscle may contribute more power to ventral expansion if the pectoral girdle is structurally immobile or the sternohyoid muscle is relatively large. In some species the epaxial muscles may generate most of the power for ventral expansion through the hyoid linkage (Muller, 1987). There is probably also variation in the relative importance of each expansion unit. Kinematic data from standard external view videos suggest that some species may rely

The Journal of Experimental Biology (2014) doi:10.1242/jeb.095810

predominantly on either dorsal or ventral expansion, rather than using both (e.g. Van Wassenbergh et al., 2009). The contribution of lateral expansion is unknown for many species, but probably also varies interspecifically. To understand how representative our results from largemouth bass are, we need data on expansion kinematics and muscle shortening from additional species.

Future directions: lateral expansion

We have demonstrated the importance of axial musculature in powering dorsal and ventral suction expansion, but more work remains to be done to understand the kinematics and muscle power responsible for lateral expansion. Lateral expansion has received much less study, but it is probably a major contributor to increasing buccal volume during suction expansion. The use of 3D skeletal kinematics has already allowed us to quantify non-planar motions of the dorsal and ventral functional units of expansion (e.g. lateral rotation of the neurocranium, medial rotation of the cleithrum), and can also be applied to lateral expansion. Importantly, the use of a reference point outside the feeding apparatus (i.e. the body plane) allows the motions of each functional unit to be measured independently. Examining the motions and muscle power responsible for each expansion unit may further reveal the integration of cranial and axial musculoskeletal systems during suction feeding.

MATERIALS AND METHODS

Animal care

Three largemouth bass (*Micropterus salmoides* Lacepède), Bass01, Bass02 and Bass03, with total lengths of 242, 281 and 277 mm, respectively, were obtained from Wiining Aquaculture in Gardner, Massachusetts, USA, and housed at Brown University. Fish were fed daily with a dry pellet diet, and all husbandry and experimental procedures were approved by the Brown University IACUC.

Surgical implantation

Each fish was surgically implanted with radio-opaque, tantalum spherical markers in the bones and muscles of interest. Fish were anesthetized with MS-222 (0.1 g l^{-1} for induction, 0.09 g l^{-1} for surgery). At least three markers were implanted in the neurocranium (0.8 mm diameter markers) and the left cleithrum (0.5 mm diameter markers; Fig. 11B). For Bass03, both the left and right cleithra were implanted, but only data from the right cleithrum were analyzed. For the urohyal bone, only two markers (0.5 mm diameter) were implanted. Bone markers were implanted by hand-drilling a hole the same diameter as the marker, and then pressing the marker into the hole. Because these bones are superficial, holes were drilled directly through the overlying tissue and into the bone.

Markers (0.8 mm diameter) were also implanted in the epaxial, hypaxial and sternohyoid muscles through the bore of an 18 gauge hypodermic needle. The needle was inserted directly into the muscle until the tip was at the desired location, and the marker was then pushed out of the needle tip with a trochar. The epaxial muscle was divided into 10 regions by 11 muscle markers, extending from the rostralmost tip of the epaxial muscle to the caudal edge of the second dorsal fin (Fig. 11). Markers were implanted superficially (4–6 mm from the dorsal surface) and just to the left of midsagittal. All but the three most rostral markers were paired with a contralateral marker at the same rostrocaudal location, but just to the right of midsagittal (Fig. 11A). These bilateral pairs were used to detect unilateral muscle shortening, indicating lateral bending and locomotor behavior. Three additional markers were placed deep (i.e. ventral) to three of the left-side, midbody markers, and together these six markers formed the body plane (Fig. 11B). The body plane was used as a fish-based frame of reference for measuring skeletal kinematics (see XROMM analysis, below).

Hypaxial muscles were divided into five regions by six intramuscular markers, extending from the cleithrum to the caudal edge of the anal fin (Fig. 11B). Markers were implanted superficially (4–6 mm deep) and just to the left of midsagittal. The sternohyoid muscle was implanted with two markers, but the length of this muscle was measured as the distance between markers in the rostral (urohyal) and caudal (cleithrum) bony attachment sites.

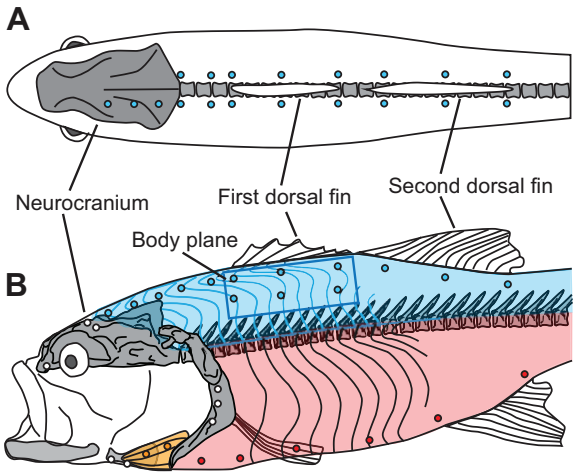

Fig. 11. Radio-opaque marker placement in the epaxial (blue), hypaxial (pink) and sternohyoid (yellow) muscles, and in the neurocranium, cleithrum and urohyal (gray). (A) Dorsal view showing left- and right-side superficial epaxial markers. (B) Left-side lateral view showing bone markers (white), sternohyoid and hypaxial muscle markers, and both superficial and deep left-side epaxial muscle markers. Six epaxial markers, three superficial and three deep, were used to define the position and motion of a mid-sagittal body plane. This body plane was used as a fish-based frame of reference for analyzing skeletal kinematics.

Surgery duration was typically ≤1 hour, and fish were given an analgesic (0.4 mg kg^{-1} butorphanol) preoperatively and an antibiotic (10 mg kg^{-1} enroflaxin) postoperatively. Fish generally recovered within 3 days, but were given at least 1 week for the markers to heal into place before feeding trials.

Feeding trials

Bass were filmed with biplanar X-ray video during suction feeding strikes on live prey. Strikes were filmed in a narrow (7×25.5×103.5 cm) tank with water no more than 15 cm deep to minimize the amount of water that the X-rays would pass through. Two X-ray machines (Imaging Systems and Service, Painesville, OH, USA) were positioned to provide approximately lateral and dorsoventral views of the fish (Fig. 3A,B). X-ray settings were 250 mA for both views, with 50–60 kVp for the lateral view and 80–90 kVp for the dorsal view machine. X-ray images were recorded with Phantom v10 high-speed cameras (Vision Research, Wayne, NJ, USA) at 1760×1760 pixel resolution, and 300 frames per second with a 1/1000 s shutter speed. Bass were offered live goldfish (*Carassius auratus*, 30-40 mm total length), and at least 10 successful strikes were recorded from each individual. Feeding trials took place over at least 2 days, and any trial where the bass showed signs of satiation was excluded. At least four resting trials (two per day) were also recorded of each bass in a still position with minimal lateral bending. X-ray images of standard grid and calibration objects were taken during each day of filming at similar settings to the feeding trials.

After all trials, fish were killed with an overdose of MS-222 and computed tomography (CT) scans were taken of each individual at 512×512 pixel resolution and 0.625 mm slice thickness (Philips Medical System, Best, The Netherlands). From these CT scans, polygonal mesh models of the neurocranium, cleithrum and bone markers were reconstructed in OsiriX (v. 3.9.2 64-bit, Pixmeo Sari Geneva, Switzerland) and Geomagic Studio (11, Geomagic, Inc. Triangle Park, NC, USA).

XROMM analysis

X-ray videos were analyzed using the XrayProject program in MATLAB (R2009a, The MathWorks, Natick, MA, USA), which is described in detail and available at xromm.org. Standard grid images were used to correct for

distortion of the videos introduced by the X-ray machine image intensifiers. Images of the calibration object with known geometry (a cube with 32 radio-opaque markers) were used to calibrate the 3D space. Marker *x*,*y*,*z* coordinates were filtered using a low-pass Butterworth filter with a 50 Hz cutoff frequency.

The precision of the XROMM marker tracking can be calculated as the standard deviation of the mean distance between two markers within a single bone during a motion sequence (Brainerd et al., 2010). Typical precision for marker-based XROMM studies is 0.1 mm. In this study, precision was ≤0.094 mm across all bass and all intraosseus marker pairs in the cleithrum and neurocranium, and the mean of all standard deviations across all feeding trials was 0.058 mm. These precision values show that the neurocranium and cleithrum are quite rigid, as deformation of either bone or movement of the markers within the bone would have generated higher standard deviation values. Additionally, errors due to bone deformation are expected to be correlated with motion of that bone (Brainerd et al., 2010), but our errors were distributed throughout each strike.

Bone marker *x*,*y*,*z* coordinates were used to calculate rigid-body translations and rotations of the neurocranium and cleithrum (Brainerd et al., 2010). Rigid-body transformations were then applied to the polygonal mesh bone models in Autodesk Maya (2010, Autodesk Inc., San Rafael, CA, USA) to animate the models with *in vivo* kinematics (Fig. 3C,D). The six markers of the body plane were treated as belonging to a single rigid body and analyzed in the same manner as bone markers. A plane was created in Maya and manually aligned to the six markers, then a rigid-body transformation based on all six markers was calculated and applied to animate the body plane.

For the urohyal, we only measured 3D translations rather than translations and rotations, as for the neurocranium and cleithrum. This study is primarily focused on the caudal translation (i.e. retraction) of the urohyal during ventral expansion. Therefore, it was only necessary to calculate the *x*,*y*,*z* translations of the urohyal, using the *x*,*y*,*z* coordinates of a single urohyal marker.

Anatomical and joint coordinate systems

The 3D kinematics of the neurocranium and cleithrum were measured relative to the body plane. For each individual, we chose the position at a frame before the start of the strike to be the zero position for the body plane and bones, and created an anatomical coordinate system (ACS) for each bone (Brainerd et al., 2010; Dawson et al., 2011; Gidmark et al., 2012). The neurocranium ACS was placed at the caudal edge of the basioccipital (Fig. 4A). The *z*-axis was oriented mediolaterally and orthogonal to both the *x*- and *y*-axes. The *y*-axis was placed midsagittally and oriented dorsovetrally so that it was parallel with the supraoccipital crest of the neurocranium. The *x*-axis was oriented rostrocaudally along the long axis of the neurocranium in the midsagittal plane, and passed through both the basioccipital foramen and the parasphenoid. The cleithrum ACS was placed at the ventral edge of the cleithrum–supracleithrum joint surface, midway between the rostral and caudal borders and the medial and lateral surfaces of the cleithrum (Fig. 4B). Again, the *z*-axis was oriented mediolaterally and defined as orthogonal to both the *x*- and *y*-axes. The *y*-axis was oriented dorsoventrally and parallel with the long axis of the dorsal cleithrum, and the *x*-axis was oriented rostrocaudally and perpendicular to the long axis of the dorsal cleithrum. For Bass03, in which the kinematics of the right cleithrum were analyzed, the cleithrum ACS was aligned as described above, but placed on the right cleithrum.

For each bone, a JCS was created from the ACS to measure translations and rotations of the bone relative to the body plane. The ACS was duplicated and one ACS attached to the body plane (the reference bone), while the other remained attached to the neurocranium or cleithrum. Rotations and translations of the JCS were calculated in a *z*, *y*, *x* order from the motion between the two ACSs. The body plane was chosen as the reference bone because it moves with the fish, but is independent of the motion of either the neurocranium or cleithrum. Both JCSs follow the right-hand rule, so positive *z*-axis motion represents translation to the fish's right and dorsal rotation, positive *y*-axis represents dorsal translation and lateral rotation, and positive *x*-axis represents rostral translation and clockwise rotation. For this study, we were primarily interested in neurocranium elevation (positive *z*-axis rotation) and cleithrum retraction (negative *z*-axis rotation).

Measurements were made of the 3D translations of the urohyal marker relative to the body plane using a single ACS placed at the anteroventral corner of the body plane, with the *x*-axis oriented rostrocaudally along the long axis of the body plane (Fig. 6A). Aligning this ACS to the body plane ensures that the axes are oriented along the rostrocadual, dorsoventral and mediolateral axes of the fish. The ACS was then attached to the body plane, which was used as the reference bone. However, instead of duplicating the ACS to form a JCS, the 3D translations of the urohyal marker were simply re-calculated relative to the ACS.

The precision of ACS and JCS translations is the same as XROMM marker tracking (0.094 mm). The precision of rotations about each axis was calculated by measuring the mean standard deviation of rotations during a resting trial when the bones were not in motion. The translational precision reflects any error resulting from marker-tracking and or bone deformation, whereas rotational precision also takes into account errors introduced during the animation process including generation and alignment of bone models from CT scans. Rotational precision differed significantly between the neurocranium and the cleithrum (*t*-test, $t=25.0$, $P<0.0001$). For the neurocranium, the mean rotational precision (across four resting trials) was <0.30 deg for all three axes and individuals, and mean precision for the cleithrum was <1.6 deg for all axes and individuals.

Fluoromicrometry

Muscle strains and shortening distances were measured from the same undistorted and calibrated videos used for the XROMM analysis. The XrayProject program in MATLAB was used to calculate the *x*,*y*,*z* coordinates of each muscle marker and all pairwise intermarker distances. Marker distances were filtered using a low-pass Butterworth filter with a 50 Hz cutoff frequency.

Marker distances from resting trials were used to confirm that intramuscular markers did not move between each day of filming. The resting length of each muscle and muscle region was calculated as the mean intermarker distance across 50 frames of a resting trial. For each fish, resting lengths were measured from four trials (two from each day), and the resting lengths were compared between the 2 days using paired *t*-tests. There was no significant change in mean resting length between filming days for any individual (Bass01 $t=0.1367$, $P=0.90$; Bass02 $t=0.98$, $P=0.33$; Bass03 $t=-0.96$, $P=0.34$).

To determine whether axial muscle shortening was due to lateral bending, we calculated the difference between left- and right-side epaxial strains. Lateral bending of the body for locomotion should be achieved by unilateral muscle shortening, whereas dorsal elevation of the neurocranium should require bilateral epaxial shortening, i.e. equal left- and right-side muscle strains. For each strike, we calculated the difference between left and right epaxial strain at the time of maximum neurocranium elevation for the whole muscle and each region. The difference in strain was generally small (means <3% for all individuals) and only the four most rostral bilateral regions had strain differences significantly different from zero (single-sample *t*-tests, region 1 $t=-3.8$, $P<0.01$; region 2 $t=5.1$, $P<0.0001$; region 3 $t=-2.3$, $P=0.05$; region 4 $t=2.4$, $P<0.05$), probably because of lateral bending of the head. To reduce any effect of lateral bending on our data, all epaxial strain and shortening magnitudes were calculated as the mean of left- and right-side values.

Muscle strain and shortening distances were calculated relative to the marker distance at the first frame of the feeding sequence. Muscle strains were calculated so that positive strain corresponded to shortening and negative strain corresponded to lengthening. For the hypaxial muscles, whole muscle strain was measured from the rostralmost to the caudalmost marker (Fig. 11B). For the epaxial muscles, the rostralmost and fourth caudalmost markers were used for whole muscle strain (Fig. 11). The three caudalmost epaxial regions were excluded because muscle length remained constant or lengthened slightly. Whole muscle strain for the sternohyoid muscle was measured from urohyal and cleithrum bone markers, which are close to the attachment sites of the sternohyoid and so represent the length of the whole muscle.

Regional muscle strains were measured within the epaxial and hypaxial muscles by calculating strain between adjacent markers in each muscle. A total of five regions were measured in the hypaxial muscles, and eight

regions in the epaxial muscles. The two rostralmost regions of the epaxial muscles were excluded, as shortening was highly variable and sometimes completely absent.

Data analysis

Kinematic and muscle length data were analyzed to describe bone motion and muscle shortening during suction expansion, as well as to test which muscles contribute power to ventral expansion and the caudal extent of axial muscle shortening. Peak neurocranium elevation (maximum *z*-axis rotation) was used as time zero to compare the timing of events to neurocranium motion. The time of peak cleithrum retraction (minimum *z*-axis rotation) was used as time zero to compare the timing of events to cleithrum motion.

To describe bone motion, we calculated peak kinematic magnitudes and timing for each bone. For the neurocranium and cleithrum, peak excursions were measured as the maximum or minimum (depending on the direction of motion) translation and rotation about each of the three JCS axes. For the urohyal, peak excursions were measured as the maximum or minimum translation along each of the three ACS axes used to describe the translation of this bone.

To describe muscle shortening, we calculated the magnitude and timing of peak muscle strain and shortening for each muscle. For whole-muscle length changes, peak magnitude and timing were calculated at maximum strain and shortening distance for each muscle. For regional strains within the epaxial and hypaxial muscles, peak strain was measured at the time of peak neurocranium elevation (for the epaxials) or peak cleithrum retraction (for the hypaxials). Maximum regional strains within both muscles usually occurred close to their respective time zeros, so this method still provides a good representation of strain magnitude while allowing us to compare strain within each muscle at the same time point.

We then compared the magnitude and relative timing of peak kinematics and muscle shortening for each bone and muscle using statistical tests. To test for differences between individuals, a one- or two-way analysis of variance (ANOVA) was performed for each variable, with individual as a random effect. Where no significant effect of individual was found, data from all three individuals were pooled. Otherwise, subsequent statistical tests were performed separately for each individual. All significant ANOVA results were followed with Tukey's HSD *post hoc* tests, and all statistical tests were performed in JMP 6.0 (SAS Institute Inc., Cary, NC, USA).

Peak timing variables were compared to neurocranium- and cleithrum-based time zeros using single-sample *t*-tests to determine if the timing of each event differed significantly from zero. The time of peak whole-muscle shortening was also compared between muscles using a two-way ANOVA to test for differences between individuals and muscles. The peak magnitudes of kinematics, muscle strain and muscle shortening were compared among bones and muscles with two-way ANOVAs. If there were significant differences between individuals, one-way ANOVAs were performed separately for each individual. Peak urohyal retraction (*x*-axis translation) and maximum hypaxial shortening were compared using a paired *t*-test, and the same was done to compare urohyal retraction and sternohyoid shortening.

Acknowledgements

We thank N. Chen, M. Langer and E. Giblin for their contributions to data collection and analysis; D. Moore for providing access to CT scanning; N. Gidmark, S. Moritz and A. Horner for assisting with X-ray filming; T. J. Roberts for providing valuable comments and discussion on the manuscript; and two anonymous reviewers for improvements to the manuscript.

Competing interests

The authors declare no competing financial interests.

Author contributions

A.L.C. designed the study, performed data collection and analysis, wrote the manuscript, and created figures. E.L.B. helped with design of the study and analysis and interpretation of results. Both authors discussed the results and edited the manuscript.

Funding

This work was supported by the Bushnell Research and Education Fund [to A.L.C.]; and the National Science Foundation [grant number 0840950 to E.L.B.].

Supplementary material

Supplementary material available online at
http://jeb.biologists.org/lookup/suppl/doi:10.1242/jeb.095810/-/DC1

References

Aerts, P. (1991). Hyoid morphology and movements relative to abducting forces during feeding in *Astatotilapia elegans* (Teleostei: Cichlidae). *J. Morphol.* **208**, 323-345.
Aerts, P., Osse, J. W. M. and Verraes, W. (1987). Model of jaw depression during feeding in *Astatotilapia elegans* (Teleostei: Cichlidae): Mechanisms for energy storage and triggering. *J. Morphol.* **194**, 85-109.
Astley, H. C. and Roberts, T. J. (2012). Evidence for a vertebrate catapult: elastic energy storage in the plantaris tendon during frog jumping. *Biol. Lett.* **8**, 386-389.
Azizi, E. and Abbott, E. M. (2013). Anticipatory motor patterns limit muscle stretch during landing in toads. *Biol. Lett.* **9**, 20121045.
Bishop, K. L., Wainwright, P. C. and Holzman, R. (2008). Anterior-to-posterior wave of buccal expansion in suction feeding fishes is critical for optimizing fluid flow velocity profile. *J. R. Soc. Interface* **5**, 1309-1316.
Brainerd, E. L., Baier, D. B., Gatesy, S. M., Hedrick, T. L., Metzger, K. A., Gilbert, S. L. and Crisco, J. J. (2010). X-ray reconstruction of moving morphology (XROMM): precision, accuracy and applications in comparative biomechanics research. *J. Exp. Zool.* **313**, 262-279.
Carroll, A. M. (2004). Muscle activation and strain during suction feeding in the largemouth bass *Micropterus salmoides*. *J. Exp. Biol.* **207**, 983-991.
Carroll, A. M. and Wainwright, P. C. (2006). Muscle function and power output during suction feeding in largemouth bass, *Micropterus salmoides*. *Comp. Biochem. Physiol.* **143**, 389-399.
Carroll, A. M. and Wainwright, P. C. (2009). Energetic limitations on suction feeding performance in centrarchid fishes. *J. Exp. Biol.* **212**, 3241-3251.
Carroll, A. M., Wainwright, P. C., Huskey, S. H., Collar, D. C. and Turingan, R. G. (2004). Morphology predicts suction feeding performance in centrarchid fishes. *J. Exp. Biol.* **207**, 3873-3881.
Coughlin, D. J. and Carroll, A. M. (2006). In vitro estimates of power output by epaxial muscle during feeding in largemouth bass. *Comp. Biochem. Physiol.* **145**, 533-539.
Dawson, M. M., Metzger, K. A., Baier, D. B. and Brainerd, E. L. (2011). Kinematics of the quadrate bone during feeding in mallard ducks. *J. Exp. Biol.* **214**, 2036-2046.
Gatesy, S. M., Baier, D. B., Jenkins, F. A. and Dial, K. P. (2010). Scientific rotoscoping: a morphology-based method of 3-D motion analysis and visualization. *J. Exp. Zool.* **313**, 244-261.
Gemballa, S. and Vogel, F. (2002). Spatial arrangement of white muscle fibers and myoseptal tendons in fishes. *Comp. Biochem. Physiol.* **133**, 1013-1037.
Gidmark, N. J., Staab, K. L., Brainerd, E. L. and Hernandez, L. P. (2012). Flexibility in starting posture drives flexibility in kinematic behavior of the kinethmoid-mediated premaxillary protrusion mechanism in a cyprinid fish, *Cyprinus carpio*. *J. Exp. Biol.* **215**, 2262-2272.
Gosline, W. A. (1977). The structure and function of the dermal pectoral girdle in bony fishes with particular reference to ostariophysines. *J. Zool.* **183**, 329-338.
Jayne, B. and Lauder, G. (1995). Are muscle fibers within fish myotomes activated synchronously? Patterns of recruitment within deep myomeric musculature during swimming in largemouth bass. *J. Exp. Biol.* **198**, 805-815.
Konow, N. and Sanford, C. P. J. (2008). Biomechanics of a convergently derived prey-processing mechanism in fishes: evidence from comparative tongue bite apparatus morphology and raking kinematics. *J. Exp. Biol.* **211**, 3378-3391.
Lauder, G. V. (1980). Hydrodynamics of prey capture by teleost fishes. In *Biofluid Mechanics* (ed. D. J. Schneck), pp. 161-181. New York, NY: Plenum Press.
Lauder, G. V. (1981). Intraspecific functional repertoires in the feeding mechanism of the characoid fishes *Lebiasina*, *Hoplias*, and *Chalceus*. *Copeia* **1981**, 154-168.
Lauder, G. V. (1982). Patterns of evolution in the feeding mechanism of actinopterygian fishes. *Am. Zool.* **22**, 275-285.
Lauder, G. V. (1985). Aquatic feeding in lower vertebrates. In *Functional Vertebrate Morphology* (ed. M. Hildebrand, D. M. Bramble, K. F. Liem, and D. B. Wake), pp. 210-229. Cambridge, MA: Harvard University Press.
Lauder, G. V. and Lanyon, L. E. (1980). Functional anatomy of feeding in the bluegill sunfish, *Lepomis macrochirus*: in vivo measurement of bone strain. *J. Exp. Biol.* **84**, 33-55.
Lauder, G. V. and Norton, S. F. (1980). Asymmetrical muscle activity during feeding in the gar, *Lepisosteus oculatus*. *J. Exp. Biol.* **84**, 17-32.
Muller, M. (1987). Optimization principles applied to the mechanism of neurocranium levation and mouth bottom depression in bony fishes (Halecostomi). *J. Theor. Biol.* **126**, 343-368.
Muller, M. (1989). A quantitative theory of expected volume changes of the mouth during feeding in teleost fishes. *J. Zool.* **217**, 639-661.
Roberts, T. J., Marsh, R. L., Weyand, P. G. and Taylor, C. R. (1997). Muscular force in running turkeys: the economy of minimizing work. *Science* **275**, 1113-1115.
Sanford, C. P. J. (2001). The novel 'tongue-bite apparatus' in the knifefish family Notopteridae (Teleostei: Osteoglossomorpha): are kinematic patterns conserved within a clade? *Zool. J. Linn. Soc.* **132**, 259-275.
Svanbäck, R., Wainwright, P. C. and Ferry-Graham, L. A. (2002). Linking cranial kinematics, buccal pressure, and suction feeding performance in largemouth bass. *Physiol. Biochem. Zool.* **75**, 532-543.
Tchernavin, V. V. (1953). *The Feeding Mechanisms of a Deep Sea Fish Chauliodus Sloani Schneider*. London: British Museum.

Thys, T. (1997). Spatial variation in epaxial muscle activity during prey strike in largemouth bass (*Micropterus salmoides*). *J. Exp. Biol.* **200**, 3021-3031.
Van Wassenbergh, S., Herrel, A., Adriaens, D. and Aerts, P. (2005). A test of mouth-opening and hyoid-depression mechanisms during prey capture in a catfish using high-speed cineradiography. *J. Exp. Biol.* **208**, 4627-4639.
Van Wassenbergh, S., Herrel, A., Adriaens, D. and Aerts, P. (2007a). Interspecific variation in sternohyoideus muscle morphology in clariid catfishes: functional implications for suction feeding. *J. Morphol.* **268**, 232-242.
Van Wassenbergh, S., Herrel, A., James, R. S. and Aerts, P. (2007b). Scaling of contractile properties of catfish feeding muscles. *J. Exp. Biol.* **210**, 1183-1193.
Van Wassenbergh, S., Lieben, T., Herrel, A., Huysentruyt, F., Geerinckx, T., Adriaens, D. and Aerts, P. (2009). Kinematics of benthic suction feeding in Callichthyidae and Mochokidae, with functional implications for the evolution of food scraping in catfishes. *J. Exp. Biol.* **212**, 116-125.
Van Wassenbergh, S., Leysen, H., Adriaens, D. and Aerts, P. (2013). Mechanics of snout expansion in suction-feeding seahorses: musculoskeletal force transmission. *J. Exp. Biol.* **216**, 407-417.
Wainwright, P. C. and Day, S. W. (2007). The forces exerted by aquatic suction feeders on their prey. *J. R. Soc. Interface* **4**, 553-560.
Westneat, M. W. (1990). Feeding mechanics of teleost fishes (Labridae; Perciformes): A test of four-bar linkage models. *J. Morphol.* **205**, 269-295.
Westneat, M. W. (2005) Skull biomechanics and suction feeding in fishes. In *Fish Biomechanics* (ed. G. V. Lauder and R. E. Shadwick), pp.29-75. London: Academic Press.